

DESIGN OF SUPERCONDUCTING PARALLEL BAR DEFLECTING AND CRABBING RF STRUCTURES*

H. Wang^{1#} and J. R. Delayen^{1,2}

¹Thomas Jefferson National Accelerator Facility, Newport News, VA 23606, U.S.A

²Old Dominion University, Norfolk, VA 23529, USA

Abstract

A new concept for a deflecting and crabbing rf structure based on half-wave resonant lines was introduced recently [1,2]. It offers significant advantages to existing designs and, because of its compactness, allows low frequency operation. This concept has been further refined and optimized for superconducting (SC) continuous wave (CW) implementation. Results of this optimization and application to a 400 MHz crabbing cavity and a 499 MHz deflecting cavity are presented.

INTRODUCTION

A new concept of rf cavity structure used for deflecting or crabbing of particle bunches has been developed recently [1,2]. One implementation is illustrated in Fig. 1. Traditional designs use the TM_{110} π -mode or operate in a $\lambda/4$ TEM mode. This design operates in a $\lambda/2$ TEM mode. The beam is kicked transversely only by electric field while perpendicularly passing between the middle of parallel bars. The parallel bars symmetrically extend $\lambda/4$ from the mid-plane to the top and bottom cavity walls, so the beam path and irises experience nearly null magnetic field. Because its characteristic size is only a half-wavelength, comparing with the TM_{110} type of cavity, the parallel bar structure is much more compact, thus allowing low frequency applications. Another distinct advantage of this structure is that the deflecting mode is the lowest frequency mode.



Figure 1: Concept of a TEM deflecting structure with curved resonant bars and variable cross-section [2].

* Authored by Jefferson Science Associates, LLC under U.S. DOE Contract No. DE-AC05-06OR23177. The U.S. Government retains a non-exclusive, paid-up, irrevocable, world-wide license to publish or reproduce this manuscript for U.S. Government purposes.

[#]haipeng@jlab.org

For superconducting cavity application, the lower order modes below the deflecting mode, like TM_{010} mode in an elliptical cavity, need to be heavily damped which can be a technical challenge. Damping the higher order modes (HOM) including the degenerate modes in parallel-bar, multi-cell structure can be done by opening waveguide slots on the cavity walls where coupling through magnetic fields is strong. We have preliminarily designed and optimized this parallel-bar cavities for two SC applications at either 2K or 4K. One is a 400 MHz cavity for future LHC's IP upgrade for local crab crossing. Another is a 499 MHz, 11 GeV beam separator for the JLab 12 GeV Upgrade project.

PARAMETER CHOICE BASED ON ANALYTICAL MODEL

The design optimization goal for a Superconducting RF (SRF) cavity is to maximize the deflecting voltage V_t (or gradient $E_t=2V_t/\lambda$, where V_t is the transverse voltage acquired by an on-crest particle) for a given surface field (E_p or B_p), i.e. to minimize E_p/E_t or B_p/E_t , and to maximize the $G \cdot R/Q$ (G is cavity's geometrical factor) toward to the low-loss concept for CW operation. An analytical model has been developed [1, 2] for the circular cross-section of the bars. When the RF loss on the side walls is substantially smaller than the loss on the bars and top/bottom walls, the ratio of peak surface electric field in the middle of bars to the deflecting gradient can be derived as the function of cylinder radius R/λ and the function of rod separation $\alpha=A/R$.

$$\frac{E_p}{E_t} = \frac{1}{4\pi} \frac{\lambda}{R} \sqrt{\frac{\alpha+1}{\alpha-1}} \exp\left[2\pi \frac{R}{A} \sqrt{\alpha^2-1}\right] \quad (1)$$

where $2A$ is the distance between the rods axes. The peak surface magnetic field at the rod joints to the top/bottom walls in this TEM structure is proportional to the peak surface electric field.

$$B_p \text{ (in mT)} = \frac{10^9}{c} E_p \text{ (in mV/m)} \quad (2)$$

where c is the velocity of light in m/sec. Other geometry dependent parameters are transverse $R/Q=V_t^2/(\omega U)$ and G . Their product $G \cdot R/Q=R_t \cdot R_s$. Here $R_t=V_t^2/P$, R_s is surface resistance of structure material. P is cavity's surface loss and U is cavity's stored energy.

$$R_t/Q = 4Z_0 \frac{\exp\left[-4\pi \frac{R}{A} \sqrt{\alpha^2-1}\right]}{\cosh^{-1}(\alpha)} \quad (3)$$

where Z_0 is the vacuum impedance $\sqrt{\epsilon_0/\mu_0} \cong 376.7\Omega$.

$$G = QR_s = 2\pi Z_0 \frac{R}{\lambda} \frac{\cosh^{-1}(\alpha)}{8 \frac{R}{\lambda} \cosh^{-1}(\alpha) + \frac{\alpha}{\sqrt{\alpha^2 - 1}}} \quad (4)$$

The universal curves (1)-(4) indicate that when $R/\lambda < 0.05$, E_p/E_t (or B_p/E_t) quickly increases when using thinner rods (see Figs. 2 and 3). $G \cdot R/Q$ is peaked at $R/\lambda = 0.05$ (see Fig. 4). Both cases are in favor of a smaller separation of A/R . We used $R/\lambda = 0.05$ and $A/R = 1.6$ as the start points of our parameter optimization in CST Microwave Studio® simulations.

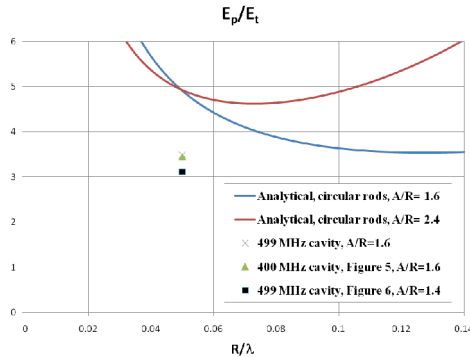


Figure 2: Ratios of peak surface electric field to transverse deflecting gradient compared from analytical to cavity designs. R is the radius of the cylindrical rods (analytical) or racetrack radius (cavity bar). $2A$ is the distance between their closest axes.

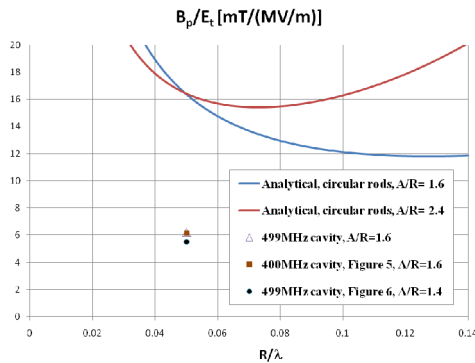


Figure 3: Ratios of peak surface magnetic field to transverse deflecting gradient compared from analytical to cavity designs.

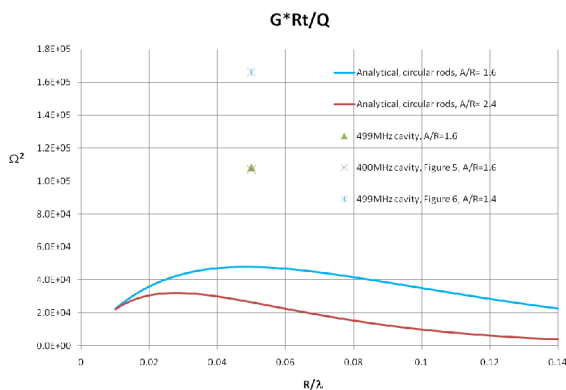


Figure 4: $G \cdot R/Q$ values compared from analytical to cavity designs.

SIMULATION EXTENSIONS AND OPTIMIZATIONS

One extension beyond the analytical optimization is to change the cross section of the parallel bars from a circle to a racetrack shape. Bar width extension in the beam travel direction will necessarily increase the beam transit time factor due to the transverse electric field peak gets extended interaction with the beam thus the R/Q gets increased. Meanwhile, a larger cross-section than a circle will reduce both surface E/M fields. Another modification is to use curved bars like shown in Figure 1. The bars would be closest at their center but bending away from each other as they near the top and bottom walls.

Analytical model of parallel bars also predicts the degenerated mode number would be as same as the bar number. There is a TEM 0-mode (acceleration) in one pair of parallel-bars above the TEM π -mode (deflection) in frequency. Introduction of beam pipes and rounding the cavity box corners plus above modifications will push the 0-mode in a larger mode separation which makes the damping HOMs easier.

In simulation, the length of outer box excluding beam pipe was fixed at $\lambda/2$ long. The width of box for the 400 MHz cavity was constrained by the beam line separation at the IP4 location on LHC. A 500 mm was used for this cavity width and could be made smaller or built a bump on the inner wall to allow other cold beam pipeline running through. A 400 mm was used for the 499 MHz cavity's box width. The curved resonance bars will lower the 0-mode frequency down than the straight bars when both types are in $\lambda/2$ height since actual curved bars are longer. A reduced bars height can make up the frequency. Such a reduction could be 15% less than the $\lambda/2$ height for $A/R = 1.6$. The final frequency was tuned by trimming bars' height to be within 1MHz of the design value. Then the E_p/E_t , B_p/E_t and $G \cdot R/Q$ values were compared and optimized. After the optimization by CST Microwave Studio®, we further confirmed the surface field values by Omega3P [3] since we believe it gives more accurate result on the surface fields than other codes [4].

DESIGN COMPARISON

Preliminary design optimization for two applications has been carried out. Their scale to the frequency is about the same. For the 499 MHz's cavity, beam aperture diameter could be made smaller (24 mm) or $A/R = 1.4$. Both E_p/E_t and B_p/E_t values are slightly lower than 400 MHz's and the $G \cdot R/Q$ value is higher. (Figures 2 to 4). For the 400 MHz's cavity, beam aperture diameter requires larger in the LHC IP4 location [5]. We used 45 mm or $A/R = 1.6$. If the A/R ratio needs larger, both E_p/E_t and B_p/E_t values are expected higher than listed in Table 1. In Table 1, we compare this cavity's properties with KEKB's squashed elliptical cavity which is in operation since 2007 [6]. Figure 5 shows the 400 MHz's cavity geometry and its surface magnetic field distribution on one of the parallel-bars. Figure 6 shows the 499 MHz's

cavity geometry cross-section and its surface electric field distribution on the parallel-bars. In Table 2, we compare this cavity's properties with JLab's CEBAF separator cavity which is the 4-rod type, $\lambda/2$ long in each cell, operating in normal conducting (NC) since 1992 [7].

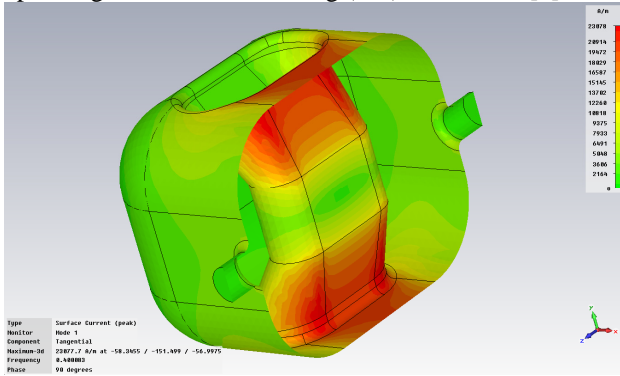


Figure 5: Surface magnetic field distributed on one of parallel-bars in the 400MHz's cavity.

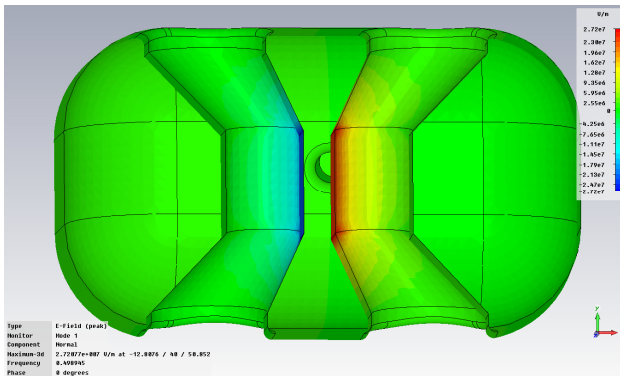


Figure 6: Surface electric field distributed between two parallel-bars in the 499 MHz's cavity.

Table 1: Properties of parallel-bar structure shown in Figure 5 calculated from Omega3P and comparison with KEKB's squashed elliptical cavity.

Parameter	Fig. 5	KEKB	Unit
Freq. of deflecting mode	400	508.9	MHz
$\lambda/2$ of deflecting mode	374.7	294.5	mm
Freq. of next higher mode	567.3	~700	MHz
Cavity active length	374.7	294.5	mm
Cavity width	500	866	mm
Cavity height	381.9	483	mm
Bars radius (R)	37.5	-	mm
Bars axes separation ($2A$)	120	-	mm
Aperture dia. ($2A-2R$)	45	188	mm
Deflecting voltage V_t^*	0.375	0.295	MV
Peak surface E-field E_p^*	3.59	4.24	MV/m
Peak surface B-field B_p^*	6.15	12.22	mT
Stored energy U^*	0.045	0.581	J
Geometry factor G	86.02	220	Ω
Transverse R/Q	1242.9	46.7	Ω

* at $E_t=1\text{MV/m}$

This is not a final design yet for each application. Further design change and optimization need to be done in more detail. For example, the coupled beam bunch stability on the LHC requires the external Q of all LOM, SOM HOM modes on the crab cavity be less than 200. A damping scheme by opening a waveguide slot on the parallel bars or on the cavity wall could be developed. For the CEBAF 11GeV's beam separation, HOM damping might be not needed but a cost benefit over the NC design has to be evaluated [8].

Table 2: Properties of parallel-bar structure shown in Figure 6 calculated from Omega3P and comparison with CEBAF's separator cavity.

Parameter	Fig. 6	CEBAF	Unit
Freq. of deflecting mode	499	499	MHz
$\lambda/2$ of deflecting mode	300.4	300.4	mm
Freq. of next higher mode	778.5	~537	MHz
Cavity active length	300.4	~300	mm
Cavity width	400	292	mm
Cavity height	233.1	292	mm
Bars radius (R)	30	10	mm
Bars axes separation ($2A$)	84.1	35	mm
Aperture dia. ($2A-2R$)	24.1	15	mm
Deflecting voltage V_t^*	0.300	0.300	MV
Peak surface E-field E_p^*	3.14	3.39	MV/m
Peak surface B-field B_p^*	5.56	8.87	mT
Stored energy U^*	0.0133	0.0012	J
Geometry factor G	75.6	34.9	Ω
Transverse R/Q	2159.8	24921	Ω

* at $E_t=1\text{MV/m}$

SUMMARY

Design of a parallel-bars structure for deflecting or crabbing cavity has been preliminary developed from its analytical concept to a realistic 3-D model for two SC applications. Its advantage over existing low frequency operation cavities has been compared.

REFERENCES

- [1] J. R. Delayen and H. Wang, Proc. LINAC 2008.
- [2] J. R. Delayen and H. Wang, submitted to PRSTAB.
- [3] K. Ko *et al.*, Physica C **441**, 258 (2006).
- [4] K. Tian and H. Wang *et al.*, "Benchmarking Different Electromagnetic Codes for the High Frequency Calculation Using a Spherical Cavity", these Proc. PAC 2009.
- [5] R. Calaga *et al.*, Proc. CARE-HHH workshop, Chavannes-de-Bogis, Nov., 2008.
- [6] K. Hosoyama *et al.*, Proc. EPAC08, p2927.
- [7] R. Kazimi *et al.*, Proc. PAC 1993, p 1109.
- [8] J. Delayen *et al.*, "Options for an 11 GeV RF Beam Separator for the Jefferson Lab CEBAF Upgrade", these Proc. PAC 2009.